PHYSICAL REVIEW D **95,** 034036 (2017)

Central production of ρ^0 in pp collisions with single proton diffractive dissociation at the LHC

Piotr Lebiedowicz,[1,*] Otto Nachtmann,[2,†] and Antoni Szczurek[1,‡]

[1]*Institute of Nuclear Physics Polish Academy of Sciences, Radzikowskiego 152, PL-31-342 Kraków, Poland*

[2]*Institut für Theoretische Physik, Universität Heidelberg, Philosophenweg 16, D-69120 Heidelberg, Germany*

(Received 23 December 2016; published 28 February 2017)

We consider the $pp \to pp\rho^0\pi^0$ and $pp \to pn\rho^0\pi^+$ processes at LHC energies. Our description is based on the nonperturbative framework of tensor pomeron and tensor reggeon exchanges. We discuss the Drell-Hiida-Deck type mechanism with centrally produced ρ^0 meson associated with a very forward/backward πN system. The considered processes constitute an inelastic (nonexclusive) background to the $pp \to pp\rho^0$ reaction in the case when only the centrally produced ρ^0 meson decaying into $\pi^+\pi^-$ is measured, the final state protons are not observed, and only rapidity-gap conditions are checked experimentally. We compare our results for the $\gamma\pi^+ \to \rho^0\pi^+$ reaction with the experimental data obtained by the H1 collaboration at HERA. We present several differential distributions for the $pp \to pn\rho^0\pi^+$ reaction and estimate the size of the proton dissociative background to the exclusive $pp \to pp\rho^0$ process. The ratio of integrated cross sections for the inelastic $pp \to pN\rho^0\pi$ processes, where $pN\rho^0\pi$ stands for $pn\rho^0\pi^+$ plus $pp\rho^0\pi^0$, to the reference reaction $pp \to pp\rho^0$ is of order of (7–10)%. We present also the ratios of the ρ^0 rapidity and transverse momentum distributions for the inelastic $pp \to pN\rho^0\pi$ versus the elastic $pp \to pp\rho^0$ reaction. Our results may be used to investigate the $\gamma\pi \to \rho^0\pi$ process at LHC energies.

DOI: 10.1103/PhysRevD.95.034036

I. INTRODUCTION

The study of vector meson production in the exclusive $pp \to ppV$ reaction is one of the important programs for the LHC. So far the CDF collaboration at Tevatron [1] and the LHCb collaboration at the LHC [2–5] presented their results for "exclusive" production of the J/ψ and ψ' mesons. These vector mesons were observed through their decay into the $\mu^+\mu^-$ final state. Also the cross sections for production of Υ states were measured; see [6]. However, so far forward going protons were not measured at the LHC. Instead, the LHCb collaboration checks only the rapidity gaps around the measured vector meson. Therefore, one is not sure whether the reaction is fully exclusive or whether there are contributions from dissociation of one or both protons in the final state. In the following we shall consider as reference reaction exclusive central ρ^0 production in pp collisions (see Fig. 1)

$$p + p \to p + \rho^0 + p. \tag{1.1}$$

Here the ρ^0 is produced by the fusion of a virtual photon emitted from one proton and a pomeron plus f_{2IR} reggeon from the other proton. In the inelastic case the proton emitting the photon, or the one emitting IP, f_{2IR}, or both protons may dissociate. If these remnants from the dissociated protons have low invariant mass they constitute a background to the reaction (1.1). Experimentally this background is notoriously difficult to handle. Also from the theory point of view these breakup reactions have rarely been studied. In [7,8] the electromagnetic dissociation was estimated to be of the order of 10% (for excited states $M_X < 2$ GeV) of the exclusive cross section for J/ψ production. Here we wish to make first estimates in the case of diffractive proton excitation for ρ^0 production. That is, we shall study the case where the proton at the IP, f_{2IR} side of Fig. 1 breaks up into a $\pi^+ n$ continuum state

$$p + p \to p + \rho^0 + n + \pi^+. \tag{1.2}$$

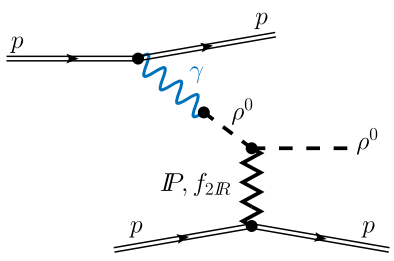

FIG. 1. Exclusive central production of ρ^0 in pp collisions by fusion of γ and IP, f_{2IR}. There is also a diagram with the role of the initial protons interchanged.

*Piotr.Lebiedowicz@ifj.edu.pl
†O.Nachtmann@thphys.uni-heidelberg.de
‡Antoni.Szczurek@ifj.edu.pl; Also at University of Rzeszów, PL-35-959 Rzeszów, Poland.

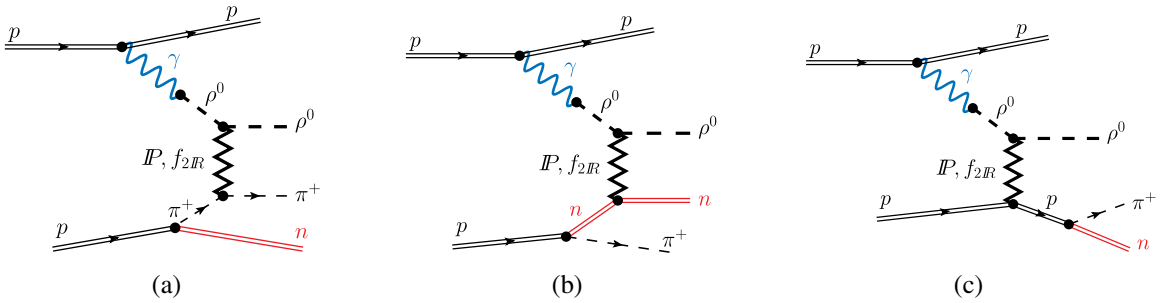

FIG. 2. The Born diagrams for processes contributing to exclusive ρ^0 meson photoproduction associated with a leading neutron in proton-proton collisions. The diagrams correspond to the Drell-Hiida-Deck type mechanism [11,12] for the pion exchange (a), neutron exchange (b), and direct production (c). In the following the incoming proton at the upper side of the diagrams will be the one with momentum p_a, at the lower side with momentum p_b. There are also the corresponding diagrams with the role of the initial protons interchanged.

The corresponding diagrams are shown in Fig. 2. This gives then a leading neutron on one side of the collision. Such leading neutrons can be rather easily detected with special forward detectors [9,10]. The reaction (1.2) can be seen as a Drell-Hiida-Deck mechanism [11,12] where a proton is dissociating into the (n, π^+) system which scatters elastically on the ρ^0 meson via the exchange of the pomeron and f_{2IR} reggeon. In addition to the pion exchange mechanism [see corresponding diagram of Fig. 2(a)] two further contributions [diagrams (b) and (c)] must be included. The two diagrams (b) and (c) give contributions to the total scattering amplitude with similar magnitude but opposite sign; see e.g. [13–18]. Therefore, in most of the phase space, in particular, at small momentum transfer squared at the $p \to n$ vertex, the contributions of diagrams (b) and (c) essentially cancel such that the contribution of diagram (a) dominates the cross section. Here we shall concentrate on the pion exchange mechanism; see Fig. 2(a). For a recent consideration of the Drell-Hiida-Deck mechanism [11,12] at LHC energies, see e.g. the discussion of the $pp \to pp\pi^0$ reaction in [19].

The production of leading neutrons was studied in deep-inelastic ep scattering (semi-inclusive $e + p \to e + n + X$ process) at HERA [20,21]. Very recently the first measurement of exclusive photoproduction of ρ^0 mesons associated with leading neutrons ($\gamma p \to \rho^0 n \pi^+$) was presented by the H1 collaboration [22]. The HERA experimental results indicate that the production of neutrons carrying a large fraction of the proton beam energy is indeed dominated by the pion exchange process. The description of these leading neutron processes still is a theoretical challenge. Exclusive processes with a leading neutron in ep collisions were discussed recently in the color dipole approach [23] using the flux of virtual pions emitted by the proton. For related work on the exclusive vector-meson (ρ, ϕ and J/ψ) production associated with a leading neutron see [24]. In the following we shall compare our results for the pion exchange mechanism [see Fig. 2(a)] with those obtained in [24].

In [25] we considered the reaction $pp \to pp(\rho^0 \to \pi^+\pi^-)$ within the tensor-pomeron approach formulated in [26]. In [27] three models for the soft pomeron, tensor, vector, and scalar, were compared with the STAR experimental data on polarized high-energy pp scattering [28]. Only the tensor-pomeron model was found to be consistent with the general rules of quantum field theory and the data from [28]. Recently, both the ρ^0-photoproduction and the purely diffractive contributions have been discussed for the $pp \to pp\pi^+\pi^-$ reaction; see [29]. In the present paper we wish to make first predictions for the process (1.2) within the same framework.

Motivated by the study of two of us of diffractive π^0-strahlung production [19] we consider here only the contributions related to a $p \to \pi^+ n$ transition which is interesting by itself (the $p \to \pi^0 p$ transition can be done analogously). A related hadronic bremsstrahlung mechanism of diffractive production of ωN states has been discussed in [30]. In general, there are also contributions due to diffractive excitation of resonances, N^* states, and their subsequent decays into the πN channel. For an analysis of proton diffractive dissociation to N^* states see [31,32].

Our paper is organized as follows. In Sec. II we present the basic formulas for the $\gamma\pi^+ \to \rho^0\pi^+$ reaction within the tensor-pomeron approach and compare our results with the H1 experimental data. In Sec. III we consider the $pp \to pn\rho^0\pi^+$ process shown in Fig. 2(a). Section IV contains numerical results for total and differential cross sections calculated for the LHC energies. We present also the ratios of the ρ^0 rapidity and transverse momentum distributions for the inelastic $pp \to pN\rho^0\pi$ processes, where $pN\rho^0\pi$ stands for $pn\rho^0\pi^+$ plus $pp\rho^0\pi^0$, versus the elastic reaction $pp \to pp\rho^0$. Section V presents our conclusions.

II. THE REACTION $\gamma\pi^+ \to \rho^0\pi^+$

As a first ingredient for our calculations we consider the reaction (see Fig. 3)

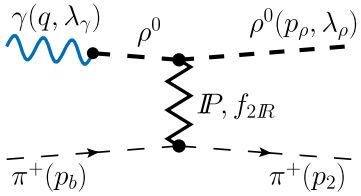

FIG. 3. Diagram for $\gamma\pi^+ \to \rho^0\pi^+$ with pomeron and f_{2IR} reggeon exchange. We use the vector meson dominance model and the corresponding relation for the $\gamma - \rho^0$ coupling.

$$\gamma(q,\lambda_\gamma) + \pi^+(p_b) \to \rho(p_\rho,\lambda_\rho) + \pi^+(p_2) \tag{2.1}$$

for real photons. Here the four-momenta and the helicities, $\lambda_\gamma = \pm 1$ and $\lambda_\rho = \pm 1, 0$, are indicated in brackets. We use standard kinematic variables

$$\begin{aligned} s &= W_{\gamma\pi}^2 = (p_b+q)^2 = (p_2+p_\rho)^2, \\ t &= (p_2-p_b)^2 = (p_\rho - q)^2. \end{aligned} \tag{2.2}$$

The differential cross section for the reaction (2.1) for unpolarized photons and no observation of the ρ^0 polarization is given by

$$\frac{d\sigma}{dt} = \frac{1}{16\pi(s-m_\pi^2)^2}\frac{1}{2}\sum_{\lambda_\gamma,\lambda_\rho}|\mathcal{M}_{\lambda_\gamma\pi^+\to\lambda_\rho\pi^+}|^2. \tag{2.3}$$

The $\mathcal{T}$-matrix element is

$$\mathcal{M}_{\lambda_\gamma\pi^+\to\lambda_\rho\pi^+} = \langle \rho^0(p_\rho,\lambda_\rho),\pi^+(p_2)|\mathcal{T}|\gamma(q,\lambda_\gamma),\pi^+(p_b)\rangle. \tag{2.4}$$

The amplitude via the tensor-pomeron exchange is written as

$$\begin{aligned} \mathcal{M}^{(IP)}_{\lambda_\gamma\pi^+\to\lambda_\rho\pi^+} &= (-i)(\epsilon^{(\rho)\mu}(p_\rho,\lambda_\rho))^* i\Gamma^{(IP\rho\rho)}_{\mu\nu\alpha\beta}(p_\rho,q) \\ &\times i\Delta^{(\rho)\nu\kappa}(q) i\Gamma^{(\gamma\to\rho)}_{\kappa\sigma}(q)\epsilon^{(\gamma)\sigma}(q,\lambda_\gamma) \\ &\times i\Delta^{(IP)\alpha\beta,\delta\eta}(s,t) i\Gamma^{(IP\pi\pi)}_{\delta\eta}(p_2,p_b), \end{aligned} \tag{2.5}$$

where $\epsilon^{(\gamma)}$ and $\epsilon^{(\rho)}$ are the polarization vectors for photon and ρ^0 meson, respectively.

The $IP\rho\rho$ vertex is given in [26] by formula (3.47).

The effective propagator of the tensor-pomeron exchange is written as (see (3.10) of [26]):

$$\begin{aligned} i\Delta^{(IP)}_{\mu\nu,\kappa\lambda}(s,t) &= \frac{1}{4s}\left(g_{\mu\kappa}g_{\nu\lambda} + g_{\mu\lambda}g_{\nu\kappa} - \frac{1}{2}g_{\mu\nu}g_{\kappa\lambda}\right) \\ &\times (-is\alpha'_{IP})^{\alpha_{IP}(t)-1} \end{aligned} \tag{2.6}$$

and fulfills the following relations

$$\begin{aligned} &\Delta^{(IP)}_{\mu\nu,\kappa\lambda}(s,t) = \Delta^{(IP)}_{\nu\mu,\kappa\lambda}(s,t) = \Delta^{(IP)}_{\mu\nu,\lambda\kappa}(s,t) = \Delta^{(IP)}_{\kappa\lambda,\mu\nu}(s,t), \\ &g^{\mu\nu}\Delta^{(IP)}_{\mu\nu,\kappa\lambda}(s,t) = 0, \qquad g^{\kappa\lambda}\Delta^{(IP)}_{\mu\nu,\kappa\lambda}(s,t) = 0. \end{aligned} \tag{2.7}$$

Here the pomeron trajectory $\alpha_{IP}(t)$ is assumed to be of standard linear form with intercept slightly above 1:

$$\begin{aligned} &\alpha_{IP}(t) = \alpha_{IP}(0) + \alpha'_{IP}t, \qquad \alpha_{IP}(0) = 1.0808, \\ &\alpha'_{IP} = 0.25\ \text{GeV}^{-2}. \end{aligned} \tag{2.8}$$

For the $IP\pi\pi$ vertex we have (see Eq. (3.45) of [26] and (B.69) of [33])

$$\begin{aligned} &i\Gamma^{(IP\pi\pi)}_{\mu\nu}(k',k) \\ &= -i2\beta_{IP\pi\pi}\left[(k'+k)_\mu(k'+k)_\nu - \frac{1}{4}g_{\mu\nu}(k'+k)^2\right] \\ &\times F_M((k'-k)^2). \end{aligned} \tag{2.9}$$

Here $\beta_{IP\pi\pi} = 1.76\ \text{GeV}^{-1}$ and $F_M(t)$ is the pion electromagnetic form factor in a parametrization valid for $t < 0$,

$$F_M(t) = \frac{1}{1 - t/\Lambda_0^2}, \tag{2.10}$$

where $\Lambda_0^2 = 0.5\ \text{GeV}^2$; see e.g. (3.22) of [34] and (3.34) of [26].

Including f_{2IR} exchange we obtain for the amplitude (2.4)

$$\begin{aligned} \mathcal{M}^{(IP+f_{2IR})}_{\lambda_\gamma\pi^+\to\lambda_\rho\pi^+}(s,t) &= ie\frac{m_\rho^2}{\gamma_\rho}\Delta_T^{(\rho)}(0)(\epsilon^{(\rho)\mu}(p_\rho,\lambda_\rho))^* \\ &\times \epsilon^{(\gamma)\nu}(q,\lambda_\gamma)V_{\mu\nu\kappa\lambda}(s,t,q,p_\rho) \\ &\times 2(p_2+p_b)^\kappa(p_2+p_b)^\lambda[F_M(t)]^2. \end{aligned} \tag{2.11}$$

Here we use (3.2), (3.10), (3.12), (3.23), (3.45), (3.47), (3.53), and (3.55) of [26], in particular, we have $M_0 \equiv 1$ GeV, $4\pi/\gamma_\rho^2 = 0.496$, $(\Delta_T^{(\rho)}(0))^{-1} = -m_\rho^2$. The function $V_{\mu\nu\kappa\lambda}(s,t,q,p_\rho)$ has the form

$$\begin{aligned} &V_{\mu\nu\kappa\lambda}(s,t,q,p_\rho) \\ &= \frac{1}{4s}\{2\Gamma^{(0)}_{\mu\nu\kappa\lambda}(p_\rho,-q)[2\beta_{IP\pi\pi}a_{IP\rho\rho}(-is\alpha'_{IP})^{\alpha_{IP}(t)-1} \\ &+ (2M_0)^{-1}g_{f_{2IR}\pi\pi}a_{f_{2IR}\rho\rho}(-is\alpha'_{IR_+})^{\alpha_{IR_+}(t)-1}] \\ &- \Gamma^{(2)}_{\mu\nu\kappa\lambda}(p_\rho,-q)[2\beta_{IP\pi\pi}b_{IP\rho\rho}(-is\alpha'_{IP})^{\alpha_{IP}(t)-1} \\ &+ (2M_0)^{-1}g_{f_{2IR}\pi\pi}b_{f_{2IR}\rho\rho}(-is\alpha'_{IR_+})^{\alpha_{IR_+}(t)-1}]\}. \end{aligned} \tag{2.12}$$

The explicit tensorial functions $\Gamma^{(i)}_{\mu\nu\kappa\lambda}(p_\rho,-q)$, $i = 0, 2$, are given in [26], formulas (3.18) and (3.19), respectively.

We take the parameters occurring in (2.12) from [26] and for the coupling constants a and b the set A given by (2.15) of [25]. In this way we described the experimental data for elastic photoproduction of ρ^0 meson in the $\gamma p \to \rho^0 p$ reaction fairly well for energies $W_{\gamma p} \gtrsim 8$ GeV; see Fig. 4 (left panel) of [25].

Figure 4(a) shows the integrated cross section for the $\gamma\pi^+ \to \rho^0\pi^+$ reaction as a function of the center-of-mass energy. Our result is compared with the H1 experimental results [22] given in Table 9 of [22] in the $W_{\gamma\pi}$ region where these data exist, see Fig. 4(b). The experimental photon-pion cross sections were extracted from the exclusive ρ^0 production associated with a leading neutron, $\gamma p \to \rho^0 n\pi^+$, using the differential cross section $d\sigma_{\gamma p}/dx_L$ and the pion flux integrated over the range $p_{t,n} < 0.2$ GeV; see [22]. We see from Fig. 4(b) that the $W_{\gamma\pi}$ shape of the data is rather well represented by our results. Note that for this it is important to have both contributions, pomeron and f_{2IR} reggeon exchange. But to obtain the normalization of the data we have to multiply our results with a factor $K = 0.6$. The same message can be determined from Fig. 4(c) where we show the ratio of cross sections for elastic ρ^0 photoproduction on pions and protons. To calculate the cross section for the $\gamma p \to \rho^0 p$ process we use formula (2.1)

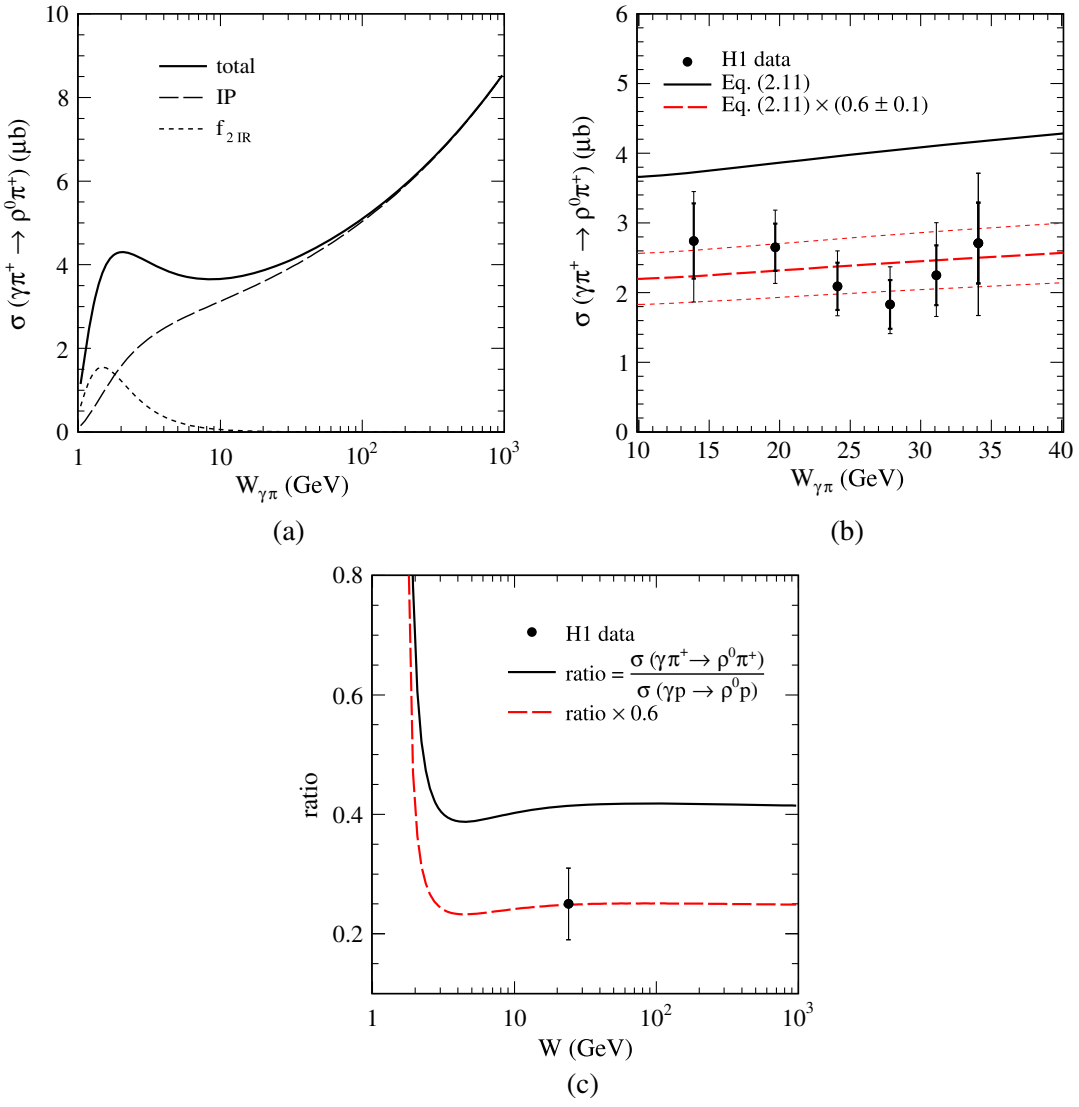

FIG. 4. (a): Cross section of elastic ρ^0 photoproduction on the pion as a function of the center-of-mass energy $W_{\gamma\pi}$. The solid line corresponds to results with both the tensor pomeron and tensor f_{2IR} exchanges. The individual pomeron and reggeon exchange contributions denoted by the long-dashed and short-dashed lines, respectively, are presented. (b): Extended view of the $W_{\gamma\pi}$ region where data from [22] exist. We show the result from (2.11) and the result multiplied by the factor 0.6 ± 0.1. The experimental data are from Table 9 of [22]. The inner error bars represent the total experimental uncertainty, the outer errors are experimental and model uncertainties are added in quadrature. (c): The ratio of cross sections $\sigma(\gamma\pi^+ \to \rho^0\pi^+)$ and $\sigma(\gamma p \to \rho^0 p)$. The data point at $W = 24$ GeV is taken from [22].

given in [25]. We can see that, according to our calculation, the ratio $\sigma^{\gamma\pi}/\sigma^{\gamma p}$ is slightly above 0.4 for $W > 20$ GeV. However, in [22] a significantly smaller value of the ratio, 0.25 ± 0.06 (at the corresponding HERA energy $\langle W \rangle = 24$ GeV), has been obtained. This inconsistency for the normalization [Fig. 4(b)] and for the ratio shown in Fig. 4(c) may come from the influence of rescattering (absorptive) corrections which may be essential for the exclusive reaction $\gamma p \to \rho^0 n \pi^+$ studied experimentally [22]. The absorption factor estimated in [22] is $K_{abs} = 0.44 \pm 0.11$ whereas we find here $K = 0.6 \pm 0.1$.

III. THE REACTION $pp \to pn\rho^0\pi^+$

Here we discuss the exclusive production of ρ^0 meson associated with a forward $\pi^+ n$ system in proton-proton collisions,

$$p(p_a,\lambda_a) + p(p_b,\lambda_b) \to p(p_1,\lambda_1) + \rho(p_\rho,\lambda_\rho) + \pi^+(p_\pi) + n(p_2,\lambda_2). \tag{3.1}$$

The kinematic variables for (3.1) are

$$\begin{aligned} q_1 &= p_a - p_1, \qquad q_2 = p_b - p_2, \\ t_1 &= q_1^2, \qquad t_2 = q_2^2, \\ \hat{s} &= (q_1+q_2)^2 = (p_\rho + p_\pi)^2, \\ \hat{t} &= (q_1 - p_\rho)^2 = (q_2 - p_\pi)^2. \end{aligned} \tag{3.2}$$

The "bare" amplitude (excluding rescattering effects) for the γIP exchange, see diagram (a) in Fig. 2, can be written as follows:

$$\begin{aligned} \mathcal{M}^{(\gamma IP)}_{\lambda_a\lambda_b\to\lambda_1\lambda_2\lambda_\rho} &= (-i)\bar{u}(p_1,\lambda_1) i\Gamma^{(\gamma pp)}_{\mu}(p_1,p_a) u(p_a,\lambda_a) \\ &\times i\Delta^{(\gamma)\mu\sigma}(q_1) i\Gamma^{(\gamma\to\rho)}_{\sigma\nu}(q_1) i\Delta^{(\rho)\nu\rho_1}(q_1) (\epsilon^{(\rho)\rho_2}(p_\rho,\lambda_\rho))^* \\ &\times i\Gamma^{(IP\rho\rho)}_{\rho_2\rho_1\alpha\beta}(p_\rho,q_1) i\Delta^{(IP)\alpha\beta,\delta\eta}(\hat{s},\hat{t}) \\ &\times i\Gamma^{(IP\pi\pi)}_{\delta\eta}(p_\pi,q_2) i\Delta^{(\pi)}(t_2) \bar{u}(p_2,\lambda_2) \\ &\times i\Gamma^{(\pi pn)}(p_2,p_b) u(p_b,\lambda_b). \end{aligned} \tag{3.3}$$

The γpp vertex is given in [26] by formula (3.26). For the pion-nucleon vertex we have

$$\begin{aligned} i\Gamma^{(\pi pp)}(p',p) &= \frac{1}{\sqrt{2}} i\Gamma^{(\pi pn)}(p',p) \\ &= -\gamma_5 g_{\pi NN} F_{\pi NN}((p'-p)^2). \end{aligned} \tag{3.4}$$

The general expressions for the pion-nucleon coupling are given in [35]. We have for the $\pi^0 pp$ coupling constant $g_{\pi NN} > 0$ and $g^2_{\pi NN}/(4\pi) = 14.4$ as a typical value quoted in the literature; see for instance [35,36]. The form factor $F_{\pi NN}(t)$ is normalized to unity at the on-shell point $F_{\pi NN}(m_\pi^2) = 1$ and parametrized here as

$$F_{\pi NN}(t) = \exp\left(\frac{t - m_\pi^2}{\Lambda^2}\right), \tag{3.5}$$

where Λ could be adjusted to experimental data. We take $\Lambda = 1$ GeV and 1.2 GeV for comparison.

In the high-energy small-angle approximation we get, including also γf_{2IR} exchange,

$$\begin{aligned} \mathcal{M}^{(\gamma IP+\gamma f_{2IR})}_{\lambda_a\lambda_b\to\lambda_1\lambda_2\lambda_\rho} &\simeq -e^2 \frac{m_\rho^2}{\gamma_\rho} (p_1+p_a)^{\rho_1} \delta_{\lambda_1\lambda_a} F_1(t_1) \\ &\times \frac{1}{t_1} \Delta_T^{(\rho)}(t_1) (\epsilon^{(\rho)\rho_2}(p_\rho,\lambda_\rho))^* \\ &\times \tilde{F}^{(\rho)}(t_1) V_{\rho_2\rho_1\alpha\beta}(\hat{s},\hat{t},q_1,p_\rho) [F_M(\hat{t})]^2 \\ &\times 2(p_\pi+q_2)^\alpha (p_\pi+q_2)^\beta \frac{F_{\pi NN}(t_2)\hat{F}_\pi(t_2)}{t_2 - m_\pi^2} \\ &\times \sqrt{2} g_{\pi NN} \bar{u}(p_2,\lambda_2)\gamma_5 u(p_b,\lambda_b). \end{aligned} \tag{3.6}$$

Here we take only the Dirac form factor of the proton $F_1(t_1)$; see (3.29) of [26]. We have also included form factors $\tilde{F}^{(\rho)}(t_1)$ and $\hat{F}_\pi(t_2)$ taking into account that the ρ created in the γ-ρ transition and the π^+ emitted from the proton $p(p_b)$, respectively, are off shell. We assume in the calculations presented in this paper that $\hat{F}_\pi(t) = F_{\pi NN}(t)$ which corresponds to the exponential form for $\hat{F}_\pi$; see (3.17) of [29]. For $\tilde{F}^{(\rho)}(t)$ we take a form as given in (B.85) of [33] with $\Lambda_\rho = 2$ GeV and $n_\rho = 0.5$; see also (3.9) and the discussion of Fig. 8 in [25].

IV. FIRST RESULTS

Now we show numerical results for the reaction $pp \to pn\rho^0\pi^+$. Our preliminary studies here are done in the Born approximation (neglecting absorptive corrections). We get the total cross section from integrating over the whole phases space: $\sigma = 387.2$ (463.2) nb at $\sqrt{s} = 7$ (13) TeV. These results are obtained for the diagram (a) of Fig. 2 plus the one with the role of the initial protons interchanged, with both IP and f_{2IR} reggeon exchanges and for $\Lambda = 1$ GeV in (3.5).[1] The realistic cross section can be obtained by multiplying the Born cross section by the corresponding gap survival factor $\langle S^2 \rangle$. In exclusive reactions, as the $pp \to pp\pi^+\pi^-$ one for instance, the gap survival factor $\langle S^2 \rangle$ is strongly dependent on the t_1 and t_2 variables, see e.g. [37]. A similar observation was made for the $pp \to ppJ/\psi$ reaction [38]. In [25] we have shown that

[1]For comparison, for $\sqrt{s} = 13$ TeV, we get the cross section equal to 407.4 nb when only the IP exchange is taken into account.

the absorption effects due to pp-interaction lead to a huge damping of the cross section for the purely diffractive mechanism ($\langle S^2\rangle \simeq 0.2$) and a relatively small reduction of the cross section for the photoproduction mechanism ($\langle S^2\rangle \simeq 0.9$). It is not clear whether such a value ($\langle S^2\rangle \simeq 0.9$) is relevant for the case of interest (3.1). Our Born-level cross section, calculated for $\sqrt{s} = 13$ TeV, should be compared with $\sigma = (206.72\text{–}278.80)$ nb obtained within the dipole saturation-inspired approach, see Table 1 of [24]. Therefore, it seems reasonable to assume that the magnitude of the absorptive corrections should be rather larger of order of 50%, $\langle S^2\rangle = 0.5$. We should emphasize that the H1 experimental group found a similar result for the $\gamma p \to \rho^0 n\pi^+$ reaction [22]. From Fig. 4(c) we find a suppression factor $\langle S^2\rangle = K \approx 0.6 \pm 0.1$. We leave a detailed analysis of absorption effects for future studies.

In Fig. 5 we show several distributions for final state particles (proton, neutron, ρ^0 meson and pion) in several kinematical variables: rapidity, pseudorapidity and Feynman-x ($x_F = 2p_z/\sqrt{s}$). Here we consider only the pion exchange mechanism and only one diagram where the photon couples to the proton $p(p_a, \lambda_a)$; see Fig. 2(a). The second diagram where the roles of the two initial protons are interchanged gives contributions which can be obtained from those presented here through the replacements $y \to -y$, $\eta \to -\eta$ and $x_F \to -x_F$. The dip in the η distribution of ρ^0 meson for $|\eta| \to 0$ is a kinematical effect; see Appendix D of [39].

From the pseudorapidity (η) distributions one can see that it is difficult to perform a fully exclusive measurement. Different types of detectors must be used: a central detector (for detection of charged pions from ρ^0 decay), very forward proton detectors (ALFA for ATLAS or TOTEM for CMS), and the zero degree calorimeters (for detection of neutrons). The π^+ meson from the reaction (3.1) shows up at rapidities $y \approx -11$ to -6.5 and is very difficult to identify with the presently available detectors.

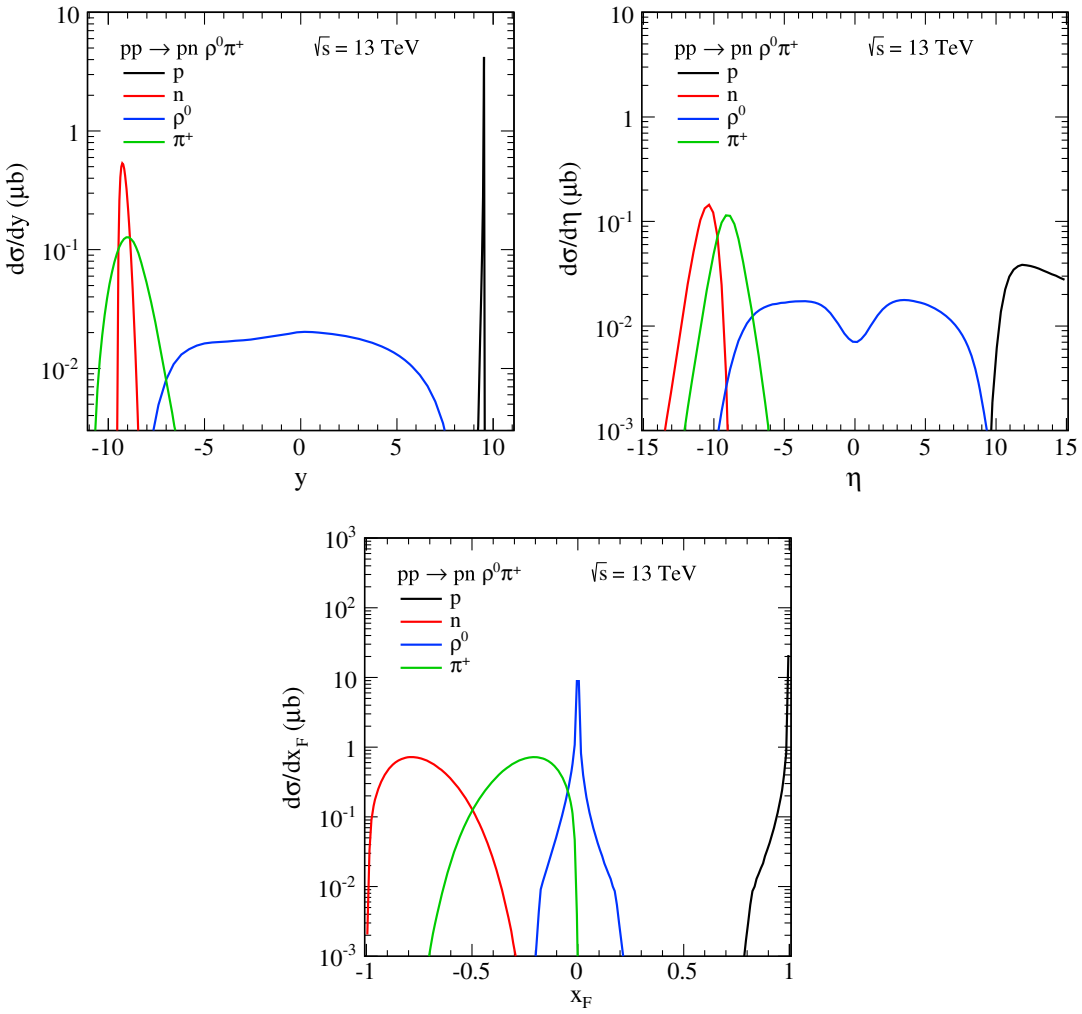

FIG. 5. The differential cross sections for the pion exchange mechanism [the diagram of Fig. 2(a)] for the reaction $pp \to pn\rho^0\pi^+$ at $\sqrt{s} = 13$ TeV. We have taken here $\Lambda = 1$ GeV in (3.5). Absorption effects are not included here.

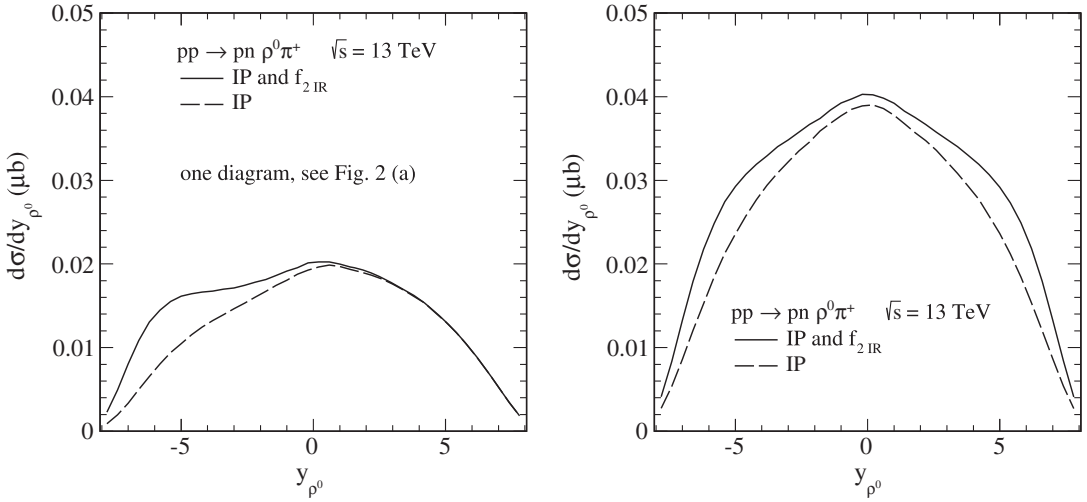

FIG. 6. The distributions in y_{ρ^0} for the reaction $pp \to pn\rho^0\pi^+$ at $\sqrt{s} = 13$ TeV. We show the Born-level calculations obtained in the pion exchange mechanism. In the left panel the results correspond to the diagram of Fig. 2(a) with tensor pomeron and f_{2IR} exchanges (the solid line) and the tensor pomeron exchange contribution alone (the long-dashed line). In the right panel we show the complete results obtained including two diagrams, Fig. 2(a) plus the one with the role of the initial protons interchanged. We have taken here $\Lambda = 1$ GeV in (3.5).

In Fig. 6 we show the rapidity distributions of ρ^0 meson produced in the pion exchange mechanism. The results shown in the left panel are obtained from the calculation taking only the diagram of Fig. 2(a) into account. In the right panel this diagram and in addition the diagram where the roles of the two initial protons are interchanged is taken into account. The solid line corresponds to the tensor pomeron and f_{2IR} exchanges while the long-dashed line corresponds to the pomeron exchange alone. One can observe in the forward/backward rapidity region an enhancement due to the inclusion of f_{2IR} exchanges. This may be an interesting point for the LHCb experimental plan in the future.[2]

Other single particle distributions are shown in Fig. 7. In the top-left panel we show the transverse momentum distributions of proton and neutron. On average protons have much smaller transverse momenta compared to neutrons. This is easy to understand as due to photon exchange protons are scattered only at small angles. In the bottom left panel we show distributions for ρ^0 meson and charged pion. Here the differences are much smaller as the ρ^0 meson feels not only photon exchange but also pomeron exchange. The four-momentum transfer squared distributions (top right panel) are shown for the $p \to p$ vertex (solid line, t_1) and for the $p \to n$ vertex (dashed line, t_2). One can observe a minimum in the t_2 distribution at $t_2 = 0$ characteristic for pion exchange. The correlations in the relative azimuthal angle between proton and neutron (solid line) and between ρ^0 meson and π^+ (dashed line) are shown in the bottom-right panel. The lack of correlation between proton and neutron can be understood as follows. The proton $p(p_a)$ emits a quasireal photon and is scattered to proton $p(p_1)$; see (3.1) and Fig. 2(a). The photon travels essentially in the direction of $\vec{p}_a$ and its polarization is determined by the azimuthal angle of $\vec{p}_1$. On the other side of the diagram of Fig. 2(a) the proton $p(p_b)$ scatters to $n(p_2)$ emitting a virtual pion $\pi^+(q_2)$. Thus, in the middle we have the reaction $\gamma\pi^+ \to \rho^0\pi^+$. Without observation of the ρ^0 polarization the cross section for this reaction is independent of the photon polarization as follows from parity invariance. Then, no information from the photon polarization and thus, from the azimuthal angle of proton $p(p_1)$, can reach the lower part of the diagram, the $p(p_b) \to n(p_2)$ transition. Therefore, the azimuthal angles of $\vec{p}_1$ and $\vec{p}_2$ should be uncorrelated, as indeed we find this from the explicit calculation; see Fig. 7, lower right panel. Also the azimuthal correlation of ρ^0 and π^+ shown in this figure can be understood from kinematics. In the $\gamma\pi^+ \to \rho^0\pi^+$ reaction at the center of the diagram of Fig. 2(a) the initial γ follows closely the direction of $\vec{p}_a$, the initial π^+ follows, not so closely but still preferentially, the direction of $\vec{p}_b$ (see Fig. 5, upper right panel). Then, in the two-body reaction $\gamma\pi^+ \to \rho^0\pi^+$ the ρ^0 and π^+ should come out preferentially at opposite azimuths, that is, at $\phi = 180°$. This is indeed what Fig. 7, lower right panel, shows.

In addition to the diagram of Fig. 2(a) there is, of course, also the diagram with the role of the initial protons interchanged. These diagrams contribute to different corners of the phase space as can be inferred from Fig. 5. Thus, there are in essence no interference effects between the amplitudes from these two diagrams. This is different for

[2]The $\pi^+\pi^-$ pairs from ρ^0 decay could be detected by the LHCb forward spectrometer which covers the region $2 < \eta < 5$. There, some experimental limitations on both outgoing pions, e.g. a cut on $p_{t,\pi} > 0.2$ GeV, must be imposed.

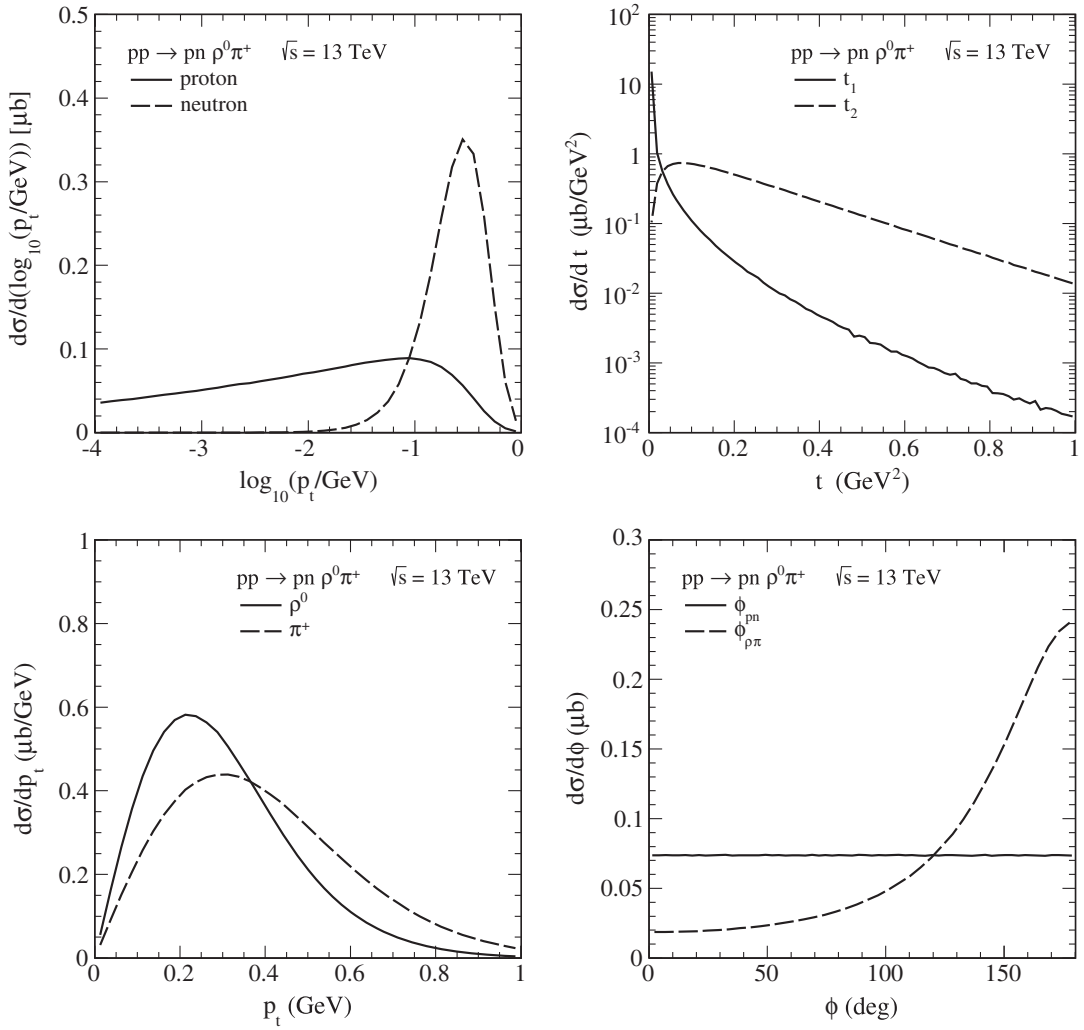

FIG. 7. Some differential cross sections for the pion exchange mechanism for the reaction $pp \to pn\rho^0\pi^+$ at $\sqrt{s} = 13$ TeV. Only the diagram of Fig. 2(a) is taken into account. Both tensor pomeron and f_{2IR} exchanges are included in the calculation. We have taken here $\Lambda = 1$ GeV in (3.5). No absorption effects are included here.

the $pp \to ppV$ processes where the two amplitudes with the photon coupling to one or the other initial proton interfere strongly. This leads, for instance, to an interesting pattern in the distribution of ϕ_{pp}, the azimuthal angle between the outgoing protons (see the discussion in [38] and also Fig. 13 of [25]).

Finally we compare the cross sections for the inelastic reactions $pp \to pn\rho^0\pi^+$ and $pp \to pp\rho^0\pi^0$ to the cross section for the exclusive elastic process $pp \to pp\rho^0$. We include here for the inelastic case the diagram Fig. 2(a) and the one with the role of initial protons interchanged and also the $pp\rho^0\pi^0$ production where the amplitude is as in (3.6) but with the factor $\sqrt{2}$ left out. For $\sqrt{s} = 13$ TeV and $\Lambda = 1$ GeV in (3.5) we get

$$\sigma_{\text{inel}} \equiv \sigma(pp \to pN\rho^0\pi) = \frac{3}{2} \times 463.2 \text{ nb} \approx 0.69\ \mu\text{b}, \tag{4.1}$$

where $pN\rho^0\pi$ stands for the $pn\rho^0\pi^+$ and $pp\rho^0\pi^0$ final states, and one of the initial protons, no matter which one, is assumed to dissociate.

For the elastic reaction we get, using the methods of [25], for $\sqrt{s} = 13$ TeV

$$\sigma_{\text{el}} \equiv \sigma(pp \to pp\rho^0) = 10.32\ \mu\text{b}. \tag{4.2}$$

For $\sqrt{s} = 7$ TeV the corresponding numbers are

$$\sigma_{\text{inel}} = 0.58\ \mu\text{b}, \qquad \sigma_{\text{el}} = 8.81\ \mu\text{b}, \tag{4.3}$$

respectively. For the ratio of inelastic and elastic cross sections we get from (4.1)–(4.3)

$$\left.\frac{\sigma_{\text{inel}}}{\sigma_{\text{el}}}\right|_{\sqrt{s}=7\text{ TeV}} \simeq 6.58 \times 10^{-2}, \tag{4.4}$$

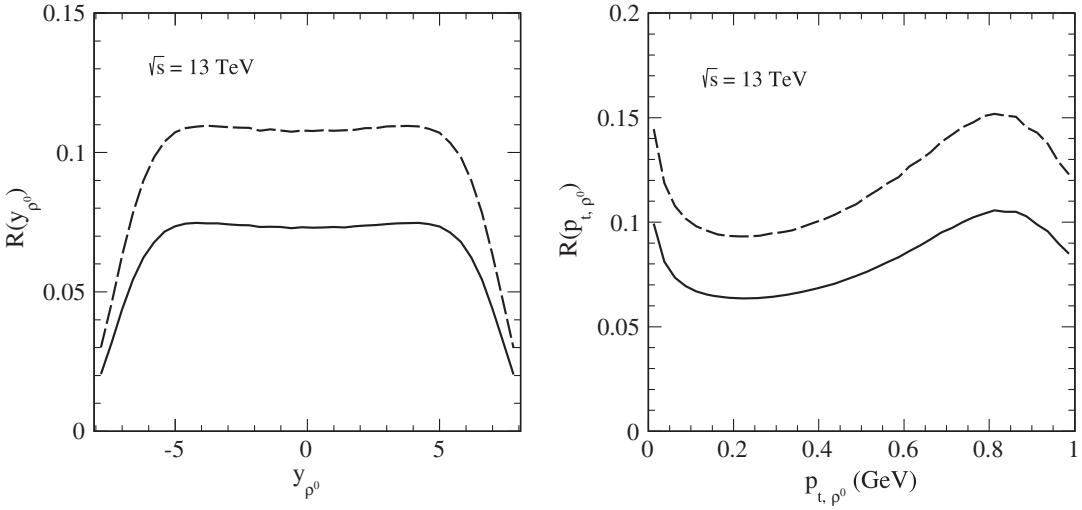

FIG. 8. The ratios $R(y_{\rho^0})$ (4.6) and $R(p_{t,\rho^0})$ (4.7) at $\sqrt{s} = 13$ TeV. The solid lines represent results for $\Lambda = 1$ GeV in (3.5) and the dashed lines are for $\Lambda = 1.2$ GeV. No absorption effects are included here but they should approximately cancel in the ratio.

$$\left.\frac{\sigma_{\rm inel}}{\sigma_{\rm el}}\right|_{\sqrt{s}=13\ \rm TeV} \simeq 6.69 \times 10^{-2}. \tag{4.5}$$

We see that this ratio increases only slightly with $\sqrt{s}$.

We must mention here that the choice of the form factor parameter Λ in (3.5) affects the size of the inelastic cross sections. For $\Lambda = 1.2$ GeV and $\sqrt{s} = 13$ TeV we get $\sigma_{\rm inel} = 1.02\ \mu$b, and $\sigma_{\rm inel}/\sigma_{\rm el} \simeq 9.88 \times 10^{-2}$. This should be compared to (4.1) and (4.5), respectively.

We are also interested how the inelastic to elastic ratio depends on rapidity and transverse momentum of the ρ^0 meson. Therefore we define

$$R(y_{\rho^0}) = \frac{d\sigma_{pp\to pN\rho^0\pi}/dy_{\rho^0}}{d\sigma_{pp\to pp\rho^0}/dy_{\rho^0}}, \tag{4.6}$$

$$R(p_{t,\rho^0}) = \frac{d\sigma_{pp\to pN\rho^0\pi}/dp_{t,\rho^0}}{d\sigma_{pp\to pp\rho^0}/dp_{t,\rho^0}}. \tag{4.7}$$

In Fig. 8 we show the ratios as a function of ρ^0 rapidity (left panel) and transverse momentum (right panel). There is almost no dependence of the ratio (4.6) on rapidity for midrapidities. Only at the edges of the rapidity phase space this ratio drops considerably. For the ratio (4.7) we predict an interesting pattern as a function of p_{t,ρ^0}.

V. CONCLUSIONS

In the present paper we have studied the reaction $pp \to pn\rho^0\pi^+$. We have considered the diagram of Fig. 2(a) with photon exchange on one side and pomeron plus f_{2IR} reggeon exchanges in the middle (between π^+ and ρ^0 meson) of the diagram. We have included also the diagram with the role of the initial protons interchanged. Due to the specificity of the reaction the corresponding amplitudes do not interfere in practice as some of the particles in the final state are emitted in different hemispheres (exclusively forward or backward) for the two diagrams. This is rather useful technically as the integration over the four-particle final state is in the case considered not easy.

We have presented first results at the Born-level. Several differential distributions have been shown explicitly for individual particles in the final state (p, n, ρ^0, π^+). Compared to the $pp \to pp\rho^0$ reaction we find no azimuthal angle correlations between the final proton and neutron for $pp \to pn\rho^0\pi^+$. Absorption effects, not considered here, may change the result slightly, however, we do not expect a large effect because the photon exchange from the proton makes the reaction fairly peripheral.

It is not clear to us whether the reaction $pp \to pn\rho^0\pi^+$ can be measured in the future at the LHC. The centrally produced ρ^0 meson could be identified by measuring two charged pions in the main ATLAS and CMS detectors. The $\pi^+\pi^-$ pairs can also be detected by the LHCb forward spectrometer. The forward and backward protons and neutrons could be measured with the help of forward proton detectors (ALFA for ATLAS or TOTEM for CMS) and the zero degree calorimeters, respectively. The very forward going π^+ is difficult to identify as there are no detectors in the corresponding region of (pseudo)rapidity.

Independent of experimental feasibility the process $pp \to pN\rho^0\pi$ is interesting on more general grounds. It was one of our motivations to study the size of the cross section and of differential distributions of the ρ^0 meson for the "inelastic" $pp \to pn\rho^0\pi^+$ compared to the reference "elastic" $pp \to pp\rho^0$ reaction. In this context we have also included the $pp \to pp\rho^0\pi^0$ "inelastic" process which gives a two times smaller contribution due to isospin symmetry of the $p \to \pi N$ vertex. We have calculated the corresponding ratios as a function of the ρ^0 rapidity and transverse

momentum. The ratio of the integrated cross sections is between 7% and 10%. For the ratios of unintegrated cross sections we found a weak dependence on ρ^0 rapidity and an interesting pattern in the ρ^0 transverse momentum dependence.

We have shown that the proton excitation processes ($pp \to pn\rho^0\pi^+$ and $pp \to pp\rho^0\pi^0$) constitute an important inelastic (nonexclusive) background to the $pp \to pp\rho^0$ reaction when the final state protons are not measured and only rapidity gap conditions are checked experimentally. The reaction $pp \to pn\rho^0\pi^+$ considered here may be a prototype for the reaction $pp \to pnJ/\psi\pi^+$. There, the mass of the J/ψ provides a (somewhat) "hard" scale. Thus, this latter reaction may also be treated in the pQCD dipole approach [24] or in the pQCD k_t-factorization approach with unintegrated gluon distributions as done e.g. in [40] for the simpler $pp \to ppJ/\psi$ process.

To summarize: in this article we have studied ρ^0 production in pp collisions where one proton undergoes diffractive excitation to an $n\pi^+$ or $p\pi^0$ system. These processes contribute in experimental studies of exclusive ρ^0 production where only large rapidity gaps around the centrally produced ρ^0 are checked but the forward and backward going protons are not detected. Recently, experimental results for this kind of processes have been published by the CDF [41] and CMS [42] collaborations. We found that ρ^0 production with single diffractive excitation of one proton (no matter which one) to $n\pi^+$ plus $p\pi^0$ constitutes $\approx$(7–10)% of the purely elastic ρ^0 production at LHC energies. This should be useful for background estimates to the elastic ρ^0 reaction. But we hope that the inelastic ρ^0 production will also be studied for its own sake in the future. Indeed, all our results depend on the $IP\rho\rho$ coupling which determines the cross section for the reaction $\gamma\pi^+ \to \rho^0\pi^+$. Thus, from a measurement of $pp \to pN\rho^0\pi$ one would be able to extract the cross section, total and differential, for $\gamma\pi \to \rho^0\pi$. This would be a continuation of the measurements of these quantities at HERA [22] at c.m. energies $W_{\gamma\pi} = 13-34$ GeV. We wish to mention that for the LHC at $\sqrt{s} = 13$ TeV one could cover a much broader range of $W_{\gamma\pi}$ but the experimental extraction of the $\gamma\pi \to \rho^0\pi$ cross sections is certainly not easy. Of course, in order to get really reliable results for $\gamma\pi \to \rho^0\pi$ in this way it would be mandatory to have control over absorptive corrections in $pp \to pN\rho^0\pi$. But this is a rather difficult subject and is definitely beyond the scope of the present paper.

ACKNOWLEDGMENTS

This research was partially supported by the Ministry of Science and Higher Education Republic of Poland (MNiSW) Grant No. IP2014 025173 (Iuventus Plus), the Polish National Science Centre Grant No. DEC-2014/15/B/ST2/02528 (OPUS), and by the Center for Innovation and Transfer of Natural Sciences and Engineering Knowledge in Rzeszów.

[1] T. Aaltonen *et al.* (CDF Collaboration), Observation of Exclusive Charmonium Production and $\gamma\gamma \to \mu^+\mu^-$ in $p\bar{p}$ Collisions at $\sqrt{s} = 1.96$ TeV, Phys. Rev. Lett. **102**, 242001 (2009).

[2] R. Aaij *et al.* (LHCb Collaboration), Exclusive J/ψ and $\psi(2S)$ production in pp collisions at $\sqrt{s} = 7$ TeV, J. Phys. G **40**, 045001 (2013).

[3] R. Aaij *et al.* (LHCb Collaboration), Updated measurements of exclusive J/ψ and $\psi(2S)$ production cross-sections in pp collisions at $\sqrt{s} = 7$ TeV, J. Phys. G **41**, 055002 (2014).

[4] (LHCb Collaboration), Reports No. LHCb-CONF-2016-007, No. CERN-LHCb-CONF-2016-007.

[5] R. McNulty, Central exclusive production at LHCb, *Proc. Sci.*, DIS2016 (2016) 181, [arXiv:1608.08103].

[6] R. Aaij *et al.* (LHCb Collaboration), Measurement of the exclusive Υ production cross-section in pp collisions at $\sqrt{s} = 7$ TeV and 8 TeV, J. High Energy Phys. 09 (2015) 084.

[7] W. Schäfer, A. Szczurek, and A. Cisek, Photoproduction of J/ψ and Υ states in exclusive and proton-dissociative diffractive events, *Proc. Sci.*, DIS2016 (2016) 205, [arXiv:1607.00900].

[8] A. Cisek, W. Schäfer, and A. Szczurek, Semiexclusive production of J/ψ mesons in proton-proton collisions with electromagnetic and diffractive dissociation of one of the protons, arXiv:1611.08210.

[9] P. Jenni, M. Nessi, and M. Nordberg (ATLAS Collaboration), Report No. CERN-LHCC-2007-001, LHCC-I-016.

[10] O. A. Grachov *et al.* (CMS Collaboration), Report No. CMS-CR-2008-038; Performance of the combined zero degree calorimeter for CMS, J. Phys. Conf. Ser. **160**, 012059 (2009).

[11] S. D. Drell and K. Hiida, Quasi-Elastic Peak in High-Energy Nucleon-Nucleon Scattering, Phys. Rev. Lett. **7**, 199 (1961).

[12] R. T. Deck, Kinematical Interpretation of the First $\pi - \rho$ Resonance, Phys. Rev. Lett. **13**, 169 (1964).

[13] V. A. Tsarev, Nucleon diffractive dissociation. I. Peripheral model with absorption, Phys. Rev. D **11**, 1864 (1975).

[14] E. L. Berger and P. Pirilä, Absorptive effects in exclusive diffraction dissociation, Phys. Rev. D **12**, 3448 (1975).

[15] L. A. Ponomarev, Description of exclusive processes in the Regge one pion exchange model, Sov. J. Part. Nucl. **7**, 70 (1976).

[16] L. A. Ponomarev, in *Proceedings, 18th International Conference on High Energy Physics, Tbilisi, USSR, Jul 15-21, 1976* (1976), p. A1, p. 24. http://inspirehep.net/record/116914/files/c76-07-15-p024.pdf.
[17] N. P. Zotov and V. A. Tsarev, Diffraction dissociation and the Drell-Hiida-Deck model, Sov. J. Part. Nucl. **9**, 266 (1978).
[18] L. Tarasiuk, Absorptive effects in nucleon diffraction dissociation, Acta Phys. Pol. B **10**, 901 (1979).
[19] P. Lebiedowicz and A. Szczurek, Exclusive $pp \to pp\pi^0$ reaction at high energies, Phys. Rev. D **87**, 074037 (2013).
[20] F. D. Aaron *et al.* (H1 Collaboration), Measurement of leading neutron production in deep-inelastic scattering at HERA, Eur. Phys. J. C **68**, 381 (2010).
[21] V. Andreev *et al.* (H1 Collaboration), Measurement of Feynman-x spectra of photons and neutrons in the very forward direction in deep-inelastic scattering at HERA, Eur. Phys. J. C **74**, 2915 (2014).
[22] V. Andreev *et al.* (H1 Collaboration), Exclusive ρ^0 meson photoproduction with a leading neutron at HERA, Eur. Phys. J. C **76**, 41 (2016).
[23] V. P. Goncalves, F. S. Navarra, and D. Spiering, Exclusive processes with a leading neutron in ep collisions, Phys. Rev. D **93**, 054025 (2016).
[24] V. P. Goncalves, B. D. Moreira, F. S. Navarra, and D. Spiering, Exclusive vector meson production with a leading neutron in photon-hadron interactions at hadronic colliders, Phys. Rev. D **94**, 014009 (2016).
[25] P. Lebiedowicz, O. Nachtmann, and A. Szczurek, ρ^0 and Drell-Söding contributions to central exclusive production of $\pi^+\pi^-$ pairs in proton-proton collisions at high energies, Phys. Rev. D **91**, 074023 (2015).
[26] C. Ewerz, M. Maniatis, and O. Nachtmann, A model for soft high-energy scattering: Tensor pomeron and vector odderon, Ann. Phys. (Berlin) **342**, 31 (2014).
[27] C. Ewerz, P. Lebiedowicz, O. Nachtmann, and A. Szczurek, Helicity in proton-proton elastic scattering and the spin structure of the pomeron, Phys. Lett. B **763**, 382 (2016).
[28] L. Adamczyk *et al.* (STAR Collaboration), Single spin asymmetry A_N in polarized proton-proton elastic scattering at $\sqrt{s} = 200$ GeV, Phys. Lett. B **719**, 62 (2013).
[29] P. Lebiedowicz, O. Nachtmann, and A. Szczurek, Central exclusive diffractive production of the $\pi^+\pi^-$ continuum, scalar, and tensor resonances in pp and $p\bar{p}$ scattering within the tensor Pomeron approach, Phys. Rev. D **93**, 054015 (2016).
[30] A. Cisek, P. Lebiedowicz, W. Schäfer, and A. Szczurek, Exclusive production of ω meson in proton-proton collisions at high energies, Phys. Rev. D **83**, 114004 (2011).
[31] L. L. Jenkovszky, O. E. Kuprash, J. W. Lämsä, V. K. Magas, and R. Orava, Dual-Regge approach to high-energy, low-mass diffraction dissociation, Phys. Rev. D **83**, 056014 (2011).
[32] L. Jenkovszky, O. Kuprash, R. Orava, and A. Salii, Low missing mass, single- and double diffraction dissociation at the LHC, Phys. At. Nucl. **77**, 1463 (2014); Odessa Astron. Pub. **25**, 102 (2012).
[33] A. Bolz, C. Ewerz, M. Maniatis, O. Nachtmann, M. Sauter, and A. Schöning, Photoproduction of $\pi^+\pi^-$ pairs in a model with tensor-pomeron and vector-odderon exchange, J. High Energy Phys. 01 (2015) 151.
[34] A. Donnachie, H. G. Dosch, P. V. Landshoff, and O. Nachtmann, Pomeron physics and QCD, Cambridge Monogr. Part. Phys., Nucl. Phys., Cosmol. **19**, 1 (2002).
[35] O. Dumbrajs, R. Koch, H. Pilkuhn, G. C. Oades, H. Behrens, J. J. de Swart, and P. Kroll, Compilation of coupling constants and low-energy parameters, Nucl. Phys. **B216**, 277 (1983).
[36] T. E. O. Ericson, B. Loiseau, and A. W. Thomas, Determination of the pion-nucleon coupling constant and scattering lengths, Phys. Rev. C **66**, 014005 (2002).
[37] P. Lebiedowicz and A. Szczurek, Revised model of absorption corrections for the $pp \to pp\pi^+\pi^-$ process, Phys. Rev. D **92**, 054001 (2015).
[38] W. Schäfer and A. Szczurek, Exclusive photoproduction of J/ψ in proton-proton and proton-antiproton scattering, Phys. Rev. D **76**, 094014 (2007).
[39] P. Lebiedowicz, O. Nachtmann, and A. Szczurek, Exclusive central diffractive production of scalar and pseudoscalar mesons; tensorial vs. vectorial pomeron, Ann. Phys. (Berlin) **344**, 301 (2014).
[40] A. Cisek, W. Schäfer, and A. Szczurek, Exclusive photoproduction of charmonia in $\gamma p \to Vp$ and $pp \to pVp$ reactions within k_t-factorization approach, J. High Energy Phys. 04 (2015) 159.
[41] T. A. Aaltonen *et al.* (CDF Collaboration), Measurement of central exclusive $\pi^+\pi^-$ production in $p\bar{p}$ collisions at $\sqrt{s} =$ 0.9 and 1.96 TeV at CDF, Phys. Rev. D **91**, 091101 (2015).
[42] (CMS Collaboration), Report No. CMS-PAS-FSQ-12-004.